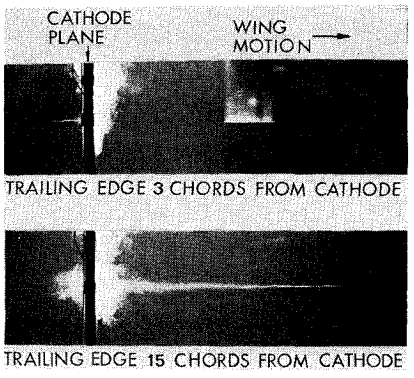

Fig 1 Axial flow patterns behind wing with square tip edge (NACA 6412 section; Reynolds number = 6.8×10^4; wing incidence = 12°).

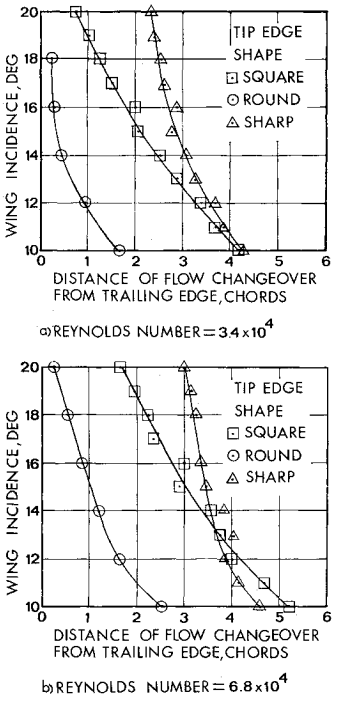

Fig 2 Position of point of changeover from axial velocity excess to axial velocity deficit behind NACA 6412 section wing.

appearance to a vortex burst. The disruption to the core by these random motions appeared to be the mechanism by which the vortex finally decayed.

Comparison with Other Experimental Results

Some of the flow features observed in the towing tank tests have been noted also in wind tunnel and other tests, using various wing sections and tip shapes, over a wide range of Reynolds numbers. For example, the tank tests have shown that, at certain stations behind a wing, an axial velocity deficit on the core centerline can change to a velocity excess as the wing incidence increases. Such a change has been observed in wind-tunnel tests by Chigier and Corsiglia.[6] The sudden change from an axial velocity excess to a velocity deficit on the core centerline has been observed in a wind-tunnel test by Scheiman, Megrail, and Shivers,[7] using smoke injected intermittently into a tip vortex. The flow distribution consisting of a centerline deficit and a core edge excess has been measured by Logan,[8] and is also apparent in towing tank photographs by Olsen.[12] Tombach[11] in flight experiments using smoke injected from a wing tip has noted a random motion along the core of apparent votex bursts, similar to the flow pattern seen in the decaying vortex in the present towing tank tests.

Conclusions

Towing tank tests have shown that the axial velocity distribution in a wing tip vortex can take the form of a centerline velocity excess, a centerline velocity deficit, or a centerline velocity combined with a core edge velocity excess. The velocity distribution at any station behind the wing depends on the wing section, tip shape, Reynolds number, wing incidence, and distance of the station from the wing. Only when these parameters are constant, can measured axial velocity distributions be compared. The shape of the streamwise tip edge appears to be particularly important. The published results of axial velocity measurements apply to a range of wing sections and tip shapes, and this may account for the variations in the axial velocity distributions.

References

[1] Olsen, J. H., Goldburg, A., and Rogers, M. (eds.), *Aircraft Wake Turbulence and Its Detection*, Plenum Press, New York, 1971.

[2] Leverton, J. W., "Helicopter Noise—Blade Slap. Part 1. Review and Theoretical Study," NASA CR-1221, Oct. 1968; "Part 2. Experimental Results," NASA CR-1983, March 1972.

[3] Ward, J. F., "Helicopter Rotor Periodic Differential Pressures and Structural Response Measured in Transient and Steady-State Maneuvers," *Journal of the American Helicopter Society*, Vol. 16, Jan. 1971, pp. 16-25.

[4] Batchelor, G. K., "Axial flow in Trailing Line Vortices," *Journal of Fluid Mechanics*, Vol. 20, Pt. 4, Dec. 1964, pp. 645-658.

[5] More, D. W. and Saffman, P. G., "Axial Flow in Laminar Trailing Vortices," *Proceedings of the Royal Society, (London)*, Vol. 33A, June 1973, pp. 491-508.

[6] Chigier, N. A. and Corsiglia, V. R., "Wind-Tunnel Studies of Wing Wake Turbulence," *Journal of Aircraft*, Vol. 9, Dec. 1972, pp. 820-825.

[7] Scheiman, J., Megrail, J. L., and Shivers, J. P., "Exploratory Investigation of Factors Affecting the Wing Tip Vortex," NASA TM-X-2516, April 1972.

[8] Logan, A. H., "Vortex Velocity Distributions at Large Downstream Distances," *Journal of Aircraft*, Vol. 8, Nov. 1971, pp. 930-932.

[9] Garodz, L. J., "Measurements of Boeing 747, Lockheed C5A and Other Aircraft Vortex Wake Characteristics by Tower Fly-by Technique," in Ref. 1, pp. 265-285.

[10] Poppleton, E. D., "Exploratory Measurements of the Flow in the Wing Tip Vortices of a Lockheed Hercules," University of Sydney, Aero. Tech. Note 7104, Dec. 1971.

[11] Tombach, I., 'Observations of Atmospheric Effects on Vortex Wake Behavior," *Journal of Aircraft*, Vol. 10, Nov. 1973, pp. 641-647.

[12] Olsen, J. H., "Results of Trailing Vortex Studies in a Towing Tank," in Ref. 1, pp. 455-472.

Analytical Solution for Inviscid Vortex Rollup from Elliptically Loaded Wings

D. K. Lezius*
Lockheed Palo Alto Research Laboratory, Palo Alto, Calif.

Introduction

THE structure of trailing vortices after rollup from aerodynamically loaded wings continues to be a subject of major interest to workers in the field of vortex research. It is desirable, for instance, to state, explicitly and analytically, the distributions of circulation and tangential velocity in the trailing vortex after rollup of the vorticity sheet that is

Received June 9, 1975. This work was partically performed under sponsorship of the National Research Council at the Large-Scale Aerodynamics Branch, NASA-Ames Research Center, Moffett Field, Calif.

Index category: Aircraft Aerodynamics (including Component Aerodynamics).

*Research Scientist. Member AIAA.

generated by the wing loading. Since experimental evidence shows the rollup process as essentially complete after several span lengths, analytical knowledge of the early vortex structure would enable one to formulate, for example, initial conditions from which subsequent vortex decay and vortex instabilities could be studied. Consideration of the axial flow in vortex cores and a variety of other phenomena associated with trailing vortices also requires that the velocity distribution after rollup be known.

The analytical difficulties associated with the vortex rollup problem were delineated by Spreiter and Sacks.[1] Because of the implicit nature of the mathematical relationships that describe the shape of an originally flat sheet of vorticity after it has rolled up into a vortex, generally valid explicit solutions do not now exist. For the mathematically simple case of parabolic wing loading, Brown[2] has given an explicit expression that approximates the circulation near the vortex center. In the more applicable cases considered by Mason and Marchman[3] and Rossow,[4] including the most interesting case of elliptical wing loading, the radial distributions of vortex circulation for complete rollup were obtained in terms of numerical solutions. The nonanalytic character of these solutions, however, renders them rather inaccessible to further analytical study.

This paper presents an explicit analytical perturbation solution that is based upon the Betz rollup theory, for the vortex circulation after rollup from wings with elliptically distributed span loading. Since the resulting series solution converges rapidly, accurate and uniformly valid results emerge for the complete rollup when only the first three terms of the expansion are retained. Further approximations that include only one term yield simple, yet accurate, expressions for the vortex circulation and the associated tangential velocity and vorticity.

Analysis

The conservation laws governing the rollup of vortex sheets from lifting wings were stated by Betz[5] about 43 years ago, but their re-emergence in simplified form and their subsequent widespread use in the field of vortex research are due to Donaldson.[6] For the benefit of the subsequent analysis, Betz's results are briefly summarized as follows: During rollup of any region of a free vortex sheet, e,g., $\eta_1 \le \eta \le 1$, into a vortex radius r_1, the circulation, centroid of vorticity, and moment of inertia of vorticity associated with that portion of the vortex sheet remain constant. An intermediate stage of the rollup process in shown in Fig. 1.

In the present notation, the nondimensional wing and vortex coordinates are $\eta = 2y/b$ and $r = 2r'/b$, with y and r' the respective physical dimensions and b the wing span. The normalized wing and vortex circulations are denoted by $\Gamma_w(\eta)$ and $\Gamma_v(r)$, respectively. The conservation statements are valid under the assumptions of inviscid rollup of the vorticity sheet into a vortex with eventually circular streamlines and no axial flow. Furthermore, for elliptically loaded wings, the concentration of vorticity at the wing tip, $|\Gamma_w/d\eta| \to \infty$ as $\eta \to 1$, assures that rollup starts at the wing tip and proceeds inward. Although the energy associated with the induced drag, as pointed out by Moore and Saffman,[7] is not conserved in the kinetic energy of the vortex pair after rollup, according to Betz's theory, the usually good agreement of the numerical solutions with experimental data seems to indicate that the error is not serious.

Thus, conservation of the three quantities stated above requires that

$$\int_1^{\eta_1} \frac{d\Gamma_w}{d\eta}\, d\eta = \int_0^{r_1} \frac{d\Gamma_v}{dr}\, dr \tag{1}$$

$$\bar{\eta}_1 = \frac{1}{\Gamma_w(\eta_1)} \int_1^{\eta_1} \frac{d\Gamma_w}{d\eta}\, \eta\, d\eta = \text{constant} \tag{2}$$

$$\int_1^{\eta_1} \frac{d\Gamma_w}{d\eta}\, (\eta - \bar{\eta}_1)^2 d\eta = \int_0^{r_1} \frac{d\Gamma_v}{dr}\, r^2 dr \tag{3}$$

From Eqs. (1) and (3), it is found that, generally

$$\Gamma_v(r_1) = \Gamma_w(\eta_1) \tag{4}$$

and

$$r_1 = \bar{\eta}_1 - \eta_1 \tag{5}$$

Substitution for arbitrary $\bar{\eta}_1$ from Eq. (2) into Eq. (5) and integration by parts yields for the corresponding vortex radius

$$r_1 = \frac{1}{\Gamma_w(\eta_1)} \int_{\eta_1}^{1} \Gamma_w(\eta)\, d\eta \tag{6}$$

Clearly, an explicit solution for η_1 in terms of r_1 would provide the desired vortex circulation $\Gamma_v(r)$.

For elliptical wing loading†, where

$$\Gamma_w(\eta) = (1 - \eta^2)^{1/2} \tag{7}$$

integration of Eq. (6) yields (for simplicity, the subscript on r and η is dropped)

$$r = \tfrac{1}{2}\left[(1-\eta^2)^{-1/2} \cos^{-1}\eta - \eta\right] \tag{8}$$

By setting $\eta = 0$, the distance from the wing centerline to the centroid of vorticity for the entire half span is recovered, and hence the radius of the area into which this vorticity rolls up, i.e., $r = \pi/4$.

So far, Eq. (8) is an exact solution of Eqs. (1-3), and any approximations necessary to obtain a solution $\eta(r)$ will reflect only the accuracy of the mathematical approximations. Thus, by letting $\theta = \cos^{-1}\eta$ (see also Jordan[8])

$$r = \tfrac{1}{2}\left[\theta(\sin\theta)^{-1} - \cos\theta\right] \tag{9}$$

can be obtained. Considering, for the moment, that only a narrow strip of vorticity near the wing tip rolls up, r can be expanded for small θ in a series whose truncated part converges sufficiently fast if η is chosen sufficiently close to 1. Upon substitution of the series representations of $\sin\theta$ and $\cos\theta$ into Eq. (9) and collecting terms after long division, the following results

$$r = \frac{1}{3}\theta^2 - \frac{1}{90}\theta^4 + \frac{13}{7560}\theta^6 - \ldots \tag{10}$$

The rapid convergence of Eq. (10) makes it apparent that the series represents r for larger values of θ (smaller η) than those originally assumed, meaning also that Eq. (10) describes the rollup of a wider vortex sheet. For example, at a point near the center of the half span, where $\eta = 0.54$ and $\theta = 1$, estimates for the lower and upper bounds of the sum of Eq. (10) can be inferred. In this case

$$\tfrac{1}{3}\sum_{n=0}^{\infty}\left(\frac{-1}{3^2}\right)^n < r < \tfrac{1}{3}\sum_{n=0}^{\infty}\left(\frac{1}{3^2}\right)^n$$

or $0.3 < r < 0.375$, whereas Eq. (9) yields the exact value of $r = 0.324$. In fact, Eq. (10) converges uniformly in the interval

†An approximate expression for $\Gamma_v(r)$ from elliptically loaded wings was given by Betz. In terms of the nondimensional vortex radius

$$\Gamma_v(r) = [3r - (9/4)r^2]^{1/2} \quad 0 < r < \tfrac{2}{3}$$
$$= 1 \quad r > \tfrac{2}{3}$$

This approximation somewhat reduces the maximum radius into which the wing vorticity rolls up.

Table 1 Exact and approximate solutions for vortex circulation $\Gamma_v(r)$

1	2	3	4	5	6	7	8
r	η Exact	η Eq. (11)	$\Gamma_v(r)$ Exact	$\Gamma_v(r)$ Eq. (12)	$\Gamma_v(r)$ Two terms Eq. (12)	$\Gamma_v(r)$ One term Eq. (12)	$\Gamma_v(r)$ One term Eq. (15)
0	1.0	1.0	0	0	0	0	0
0.2	0.7096	0.7096	0.705	0.705	0.705	0.699	0.712
0.4	0.4412	0.4403	0.897	0.898	0.899	0.889	0.900
0.6	0.1987	0.1945	0.980	0.981	0.982	0.974	0.980
0.78	0.0054	−0.0056	1.0	1.0	1.0	0.999	1.0
$\pi/4$	0	−0.0112	1.0	1.0	1.0	0.999	1.0

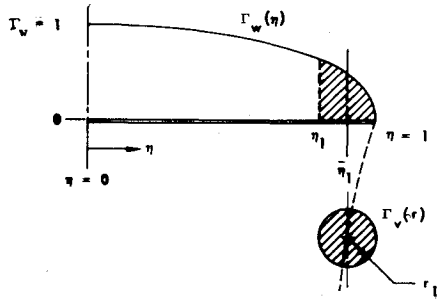

Fig. 1 Rollup of a free vortex sheet.

$0 \le \theta \le \pi/2$, so that the expression for r remains valid for rollup of the entire vortex sheet from $\eta = 1$ to $\eta = 0$. The only error introduced will be that of truncation, determined by the choice to retain the first three terms of the series.

Reversion of the truncated series in Eq. (10) and substitution of $\theta = \cos^{-1}\eta$ gives $\eta(r)$ explicitly, thus:

$$\eta = \cos[3r + \frac{3}{10} r^2 - \frac{111}{1400} r^3]^{1/2} \tag{11}$$

The distribution of circulation in the vortex is obtained by combining the result of Eq. (11) with Eqs. (4) and (7)

$$\Gamma_v(r) = \sin[3r + \frac{3}{10} r^2 - \frac{111}{1400} r^3]^{1/2} \tag{12}$$

the units of the square root being in radians. As shown in Table 1, the expression thus derived provides rather accurate values for the vortex circulation (Table 1, cols. 4 and 5). The corresponding values of η and $\Gamma_v(r)$ were rounded to four and three significant figures, respectively, whereby the exact values of η (col. 2) are solutions of Eq. (8).

For the nondimensional, inviscid velocity profile, Eq. (12) yeilds,

$$v(r) = \frac{1}{2\pi r} \sin\,(3r + \frac{3}{10} r^2 - \frac{111}{1400} r^3)^{1/2} \tag{13}$$

indicating the well-known velocity dependence in the inner region of the vortex according to $v(r) \sim r^{-1/2}$. The vorticity is given by

$$\xi(r) = \frac{dv}{dr} + \frac{v}{r} = \frac{3}{4\pi r} \frac{(1 + \frac{1}{5} r - \frac{111}{1400} r^2)}{(3r + \frac{3}{10} r^2 - \frac{111}{1400} r^3)^{1/2}}$$

$$\times \cos\,(3r + \frac{3}{10} r^2 - \frac{111}{1400} r^3)^{1/2} \tag{14}$$

This expression approximates to within 0.3% the exact solution for $\xi(r)$, which may be obtained in terms of the wing coordinate η by equating the integrants of Eq. (1). One can then evidently write

$$d\Gamma_v/dr = (d\Gamma_w/d\eta)\,(dr/d\eta)^{-1}$$

After differentiating Eq. (8), we obtain the exact relationship

$$\xi(r) = \frac{1}{2\pi r} \frac{d\Gamma_v}{dr} = \frac{\eta(1-\eta^2)^{1/2}}{\pi r(2 - \eta^2 - \eta(1-\eta^2)^{-1/2}\cos^{-1}\eta)} \tag{15}$$

It is interesting to note that Betz's approximate expression for the vortex circulation† and Eq. (12) have the same leading term in r. This results in equal values for the slope of $\Gamma_v(r)$, and thus for the vorticity $\xi(r)$ near the vortex center since, for small r, $\sin\sqrt{3r} \approx \sqrt{3r}$. In this limit, the leading term alone approaches the exact solution in both cases. A one-term approximation, however, of Betz's formula cannot be regarded as sufficiently accurate above $r \approx 0.12$. Yet, retaining only the lowest order term in r of Eq. (12) does indeed represent the vortex circulation to within 1% of the exact solution (Table 1, cols. 4 and 7) over the interval $0 \le r \le \pi/4$, and thus for the complete vortex rollup.

An alternative one-term approximation for $\Gamma_v(r)$ that is exact at $r = 0$, and also at $r = \pi/4$, is obtained by choosing the coefficient of r to be π rather than 3. Applying this approximation to Eq. (12) gives for the circulation and tangential velocity

$$\Gamma_v(r) \approx \sin\sqrt{\pi r} \tag{16}$$

and from Eq. (13)

$$v(r) \approx (1/2\pi r)\sin\sqrt{\pi r} \tag{17}$$

The corresponding expression for the radial distribution of vorticity is then given by

$$\xi(r) \approx (1/4r\sqrt{\pi r})\cos\sqrt{\pi r} \tag{18}$$

The choice of π for the lowest-order coefficient is, of course, motivated by the desire that one-term representation of Γ_v and ξ be exact at $r = \pi/4$. Although, to this approximation, $\Gamma_v(r)$ increases slightly faster for small r (Table 1, col. 8) than the exact solution, the error in this region still remains less than 1% of the exact solution for Γ_v and less than 4% for $\xi(r)$. Above $r = 0.4$, the relationship shown in Eq. (16) represents an exceedingly accurate approximation of the vortex circulation.

In conclusion, it is well to point out that the degree of approximation to inviscid vortex rollup offered by Eqs. (16-18) far outweighs that required for most engineering applications or for comparison with experimental data. The real usefulness

of these expressions lies in their mathematical simplicity, which should facilitate further analytical studies.

References

[1] Spreiter, J. R. and Sacks, A. H., "The Rolling Up of the Trailing Vortex Sheet and Its Effect on the Downwash Behind Wings," *Journal of the Aeronautical Sciences*, Vol. 18, January 1951, pp. 21-32.

[2] Brown, C. D., "Aerodynamics of Wake Vortices," *AIAA Journal*, Vol. 11, April 1973, pp. 531-536.

[3] Mason, W. H. and Marchman, J. F., III, "Far-Field Structure of Aircraft Wake Turbulence," *Journal of Aircraft*, Vol. 10, Feb. 1973, pp. 86-92.

[4] Rossow, V. J., "On the Inviscid Rolled-Up Structure of Lift Generated Vortices," NASA, TMX-62, 224, 1973.

[5] Betz, A., "Behavior of Vortex Systems," NACA TM 713; translated from *Zeitschrift fuer Angewandte Mathematik und Mechanik*, Vol. 12, 1932, pp. 164-174.

[6] Donaldson, C. duP., "A Brief Review of the Aircraft Trailing Vortex Problem," AFOSR-TR-71-1910, May 1971, Air Force Office of Scientific Research, Washington, D.C.

[7] Moore, D. W. and Saffman, P. G., "Axial Flow in Laminar Trailing Vortices," *Proceedings of the Royal Society (London)*, Ser. A., Vol. 33A, June 1973, pp. 491-508.

[8] Jordan, P. F., "Structure of Betz Vortex Cores," *Journal of Aircraft*, Vol. 10, Nov. 1973, pp. 691-693.

Effect of Aeroacoustic Interactions on Ejector Performance

Brian Quinn*
Air Force Aero-Propulsion Laboratory, Wright-Patterson, AFB, Ohio

Experimental Background

THE mass entrainment performance of a family of ejectors has been measured over a range of primary air pressures and temperatures, $0 < P_{RES} \leq 120$ psig, $60 < T_{RES} \leq 1000$°F. The ejector entrained ambient air through an efficient bellmouth inlet that led to a cylindrical mixing duct of constant diameter $D = 1.375$ in. The length, L, of the duct was varied incrementally. Primary air was injected through a long, slender, convergent nozzle whose exit plane was circular, of diameter $d = 0.2656$ in. The axes of symmetry of the duct and the nozzle were coincident, the exit plane of the nozzle and the throat of the bellmouth were also coincident.

A venturi metered the primary flow rate $\dot{m}_0$, whereas the entrained mass flow $\dot{m}_1$, was computed from measurements of ambient pressure and temperature and the pressure at the throat of the bellmouth inlet. Both devices had previously been thoroughly calibrated.[1] The mixture of primary and entrained flows exhausted to the ambient. Beginning 1.1875 in. downstream from the plane of injection, wall pressure taps were drilled at quarter inch intervals along the mixing duct. Adjacent taps were spaced at 90° intervals around the circumference of the duct.

Testing began with the longest mixing duct and proceeded to ducts of decreasing length. The performance of the longer ducts, in which mixing of the two streams was nearly complete, agreed very well with the results of a simple, one-dimensional analysis in which integral expressions of mass, momentum and energy were balanced. This can be seen in the upper curve of Fig. 1. Geometries within the interval $15.75 > L/D \geq 6.5$, roughly, produced similar results: the entrainment ratio $\dot{m}_1/\dot{m}_0$ decreased with increasing reservoir pressure ratio, although overall performance dropped slightly below the fully mixed predictions as the length of the duct decreased.

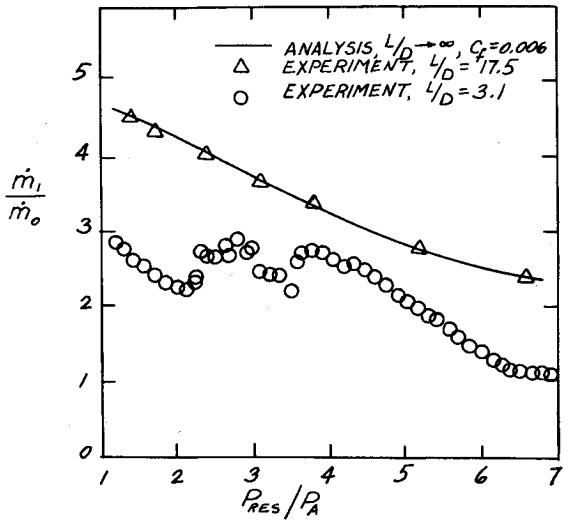

Fig. 1 Effects of reservoir pressure on mass augmentation, $T_{RES}/T_A = 1.0$.

The Anomaly

What seemed to be substantial scatter first appeared in the $L/D = 5.82$ data. It was not until testing was repeated at 2 psi increments of reservoir pressure that a real trend became obvious and was considerably amplified with the shorter ducts. Typical data are shown in Fig. 1. Performance at first followed the trend of the simple analysis, although at a substantial reduction that reflected incomplete mixing. A trend reversal occurred at approximately two atmospheres reservoir pressure and peaked at 2.7. A second peak at $P_{RES} = 3.7\,P_A$ brought the data near the fully mixed results. The peaks clearly indicate an accelerated mixing condition that persisted at the same pressure ratios with all of the ducts. This condition was not obvious in the mass entrainment data from the longer ducts because performance levels representative of nearly complete mixing were achieved at all pressure ratios. Nevertheless, accelerated mixing did occur and was obvious in the wall pressure data.

Figure 2 is typical and describes the increase in wall pressure, from P_{BM} at the bellmouth throat to P_A at the exhaust plane, along the length of the duct. In these tests only mixing and skin friction contribute to the pressure rise and the effect of the latter is small. The distance along the tube at which the data essentially become zero is therefore indicative of the rate of mixing. Three distinct mixing rates are obvious. At reservoir pressure ratios of three and less, the primary and entrained streams require approximately seven or eight duct diameters to complete mixing. In contrast, the $P_{RES}/P_A = 3.7$ data describe an accelerated mixing condition by achieving their terminal state much earlier, at $X/D = 5$. This is the same pressure ratio at which one of the mass entrainment peaks in Fig. 1 occurred. The pressure ratio 5 and 6.6 data suggest a retarded condition that requires nine duct diameters to mix completely.

A Proposed Mechanism

Research in the past decade has convincingly related entrainment and mixing to the large scale vortices convected along the outer edges of jets and wakes, a structure known to persist throughout a very large Reynolds number range. It was, therefore, perplexing that the same nozzle should issue jets with three distinct turbulence structures under similar conditions. Abrupt changes in the quality of the ejector's noise under different levels of reservoir pressure suggested an

Received August 13, 1975. The author gratefully acknowledges the technical contributions of H. Toms.

Index category: Jets, Wakes, and Viscid-Inviscid Flow Interactions.

*Research Engineer. Associate Fellow AIAA.